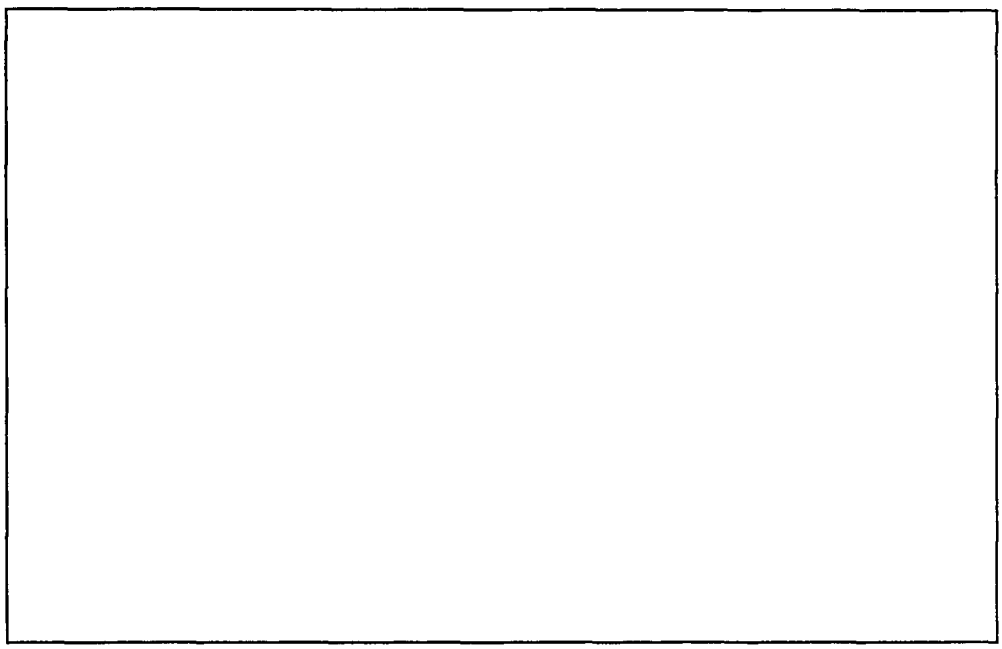

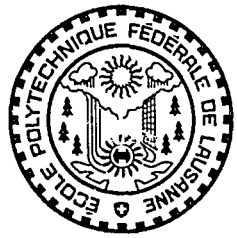

C R P P

ÉCOLE POLYTECHNIQUE FÉDÉRALE DE LAUSANNE - SUISSE

LRP 532/95 November 1995

PAPERS PRESENTED AT THE IAEA TECHNICAL COMMITTEE MEETING ON H-MODE PHYSICS Princeton University, 18 - 20 September 1995

TCV-Team

To be published in
Plasma Physics and Controlled Fusion

LIST OF CONTENTS

Ohmic H-modes in the TCV Tokamak

H. Weisen, F. Hofmann, M.J. Dutch, Y. Martin, A. Pochelon, J.-M. Moret, B.P. Duval, A. Hirt, J.B. Lister, Ch. Nieswand, R.A. Pitts, Z. A. Pietrzyk, M. Anton, R. Behn, G. Besson, F. Bühlmann, R. Chavan, D. Fasel, A. Favre, S. Franke, P. Isoz, P. Lavanchy, B. Joye, X. Llobet, P. Mandrin, B. Marletaz, Ph. Marmillod, J. C. Magnin, J.-M. Mayor, P.J. Paris, A. Perez, O. Sauter, W. van Toledo, G. Tonetti, M.Q. Tran, F. Troyon and D.J. Ward

Centre de Recherches en Physique des Plasmas
Ecole Polytechnique Fédérale de Lausanne
Association EURATOM-Confédération Suisse
CH-1015 Lausanne, Switzerland

Abstract: The TCV tokamak has obtained ohmic H-modes in virtually all diverted plasmas with the ion ∇B drift directed towards an X-point and in several elongated limiter plasmas. Troyon factors ($\beta_{tor}aB/I_p$) up to 2 and line average densities up to $2.2 \cdot 10^{20} m^{-3}$, corresponding to the Greenwald limit, have been obtained in diverted ELM-free H-modes. Quasi-stationary H-modes lasting for the entire current flat top (1.5 s) have been obtained in the presence of regular ELMs. The occurence and magnitude of ELMs have been found to depend on configurational parameters such as the position of the 'active' X-point in unbalanced Double-Null discharges and the plasma-wall separation in Single-Null discharges. These dependencies have permitted active control of ELM behaviour in TCV. A continuous spectrum of ELM amplitudes and frequencies has been observed, ranging from clearly identifiable type III ELMs to large, low frequency ELMs which expell up to 12% of the stored energy and up to 7% of the particle content and are reminiscent of type I ELMs. A previously unknown, benign kind of ELM, with a maximum amplitude in the divertor region, has also been observed.

1. Introduction

TCV (Tokamak à Configuration Variable) is a compact, highly elongated tokamak, capable of producing limited or diverted plasmas with currents up to 1 MA (Hofmann et al. 1994). The machine parameters are $R = 0.88$ m, $a \leq 0.25$ m, $B_T \leq 1.5$ T, $\kappa = b/a \leq 3$. Discharge parameters achieved are $I_p \leq 800$ kA, $-0.7 \leq \delta \leq 1$, $1 \leq \kappa \leq 2.05$, $\langle n_e \rangle \leq 2.2 \cdot 10^{20}$ m^{-3}. The main aim of TCV is to investigate effects of plasma shape, especially high elongation and high triangularity, on tokamak physics and performance. Plasma shape in TCV is controlled by sixteen independent shaping coils located between the vacuum vessel and the toroidal field coils. The vacuum vessel is a continuous structure of nearly rectangular cross section, 1.5 by 0.5 m and is protected with graphite tiles to 64% of the inside wall area.

Following the first vessel boronization in 1994, ohmic H-modes have been obtained in virtually all diverted configurations, whether Single Null (SN) or Double Null (DN), which had the ion grad_B drift towards an X-point and also in some inner wall limited plasmas (figure 1). Recently ELM-free H-modes have been observed in good vessel conditions for some SN plasmas, such as discharge 7372 in figure 1, for both directions of the ion grad_B drift. Confinement times up to 80 ms and $\beta_n = \beta_{tor}aB/I_p$ up to 2 have been obtained in diverted ELM-free H-modes, twice the highest values achieved in L-modes (Pochelon et al 1995). The highest line average density obtained is $2.2 \cdot 10^{20}$ m^{-3}, corresponding to the Greenwald limit $\langle n_e \rangle_{GL} = 0.27\ I_p/a^2$, where n_e is in units of $10^{20} m^{-3}$, I_p in MA and a in m (Greenwald et al 1988).

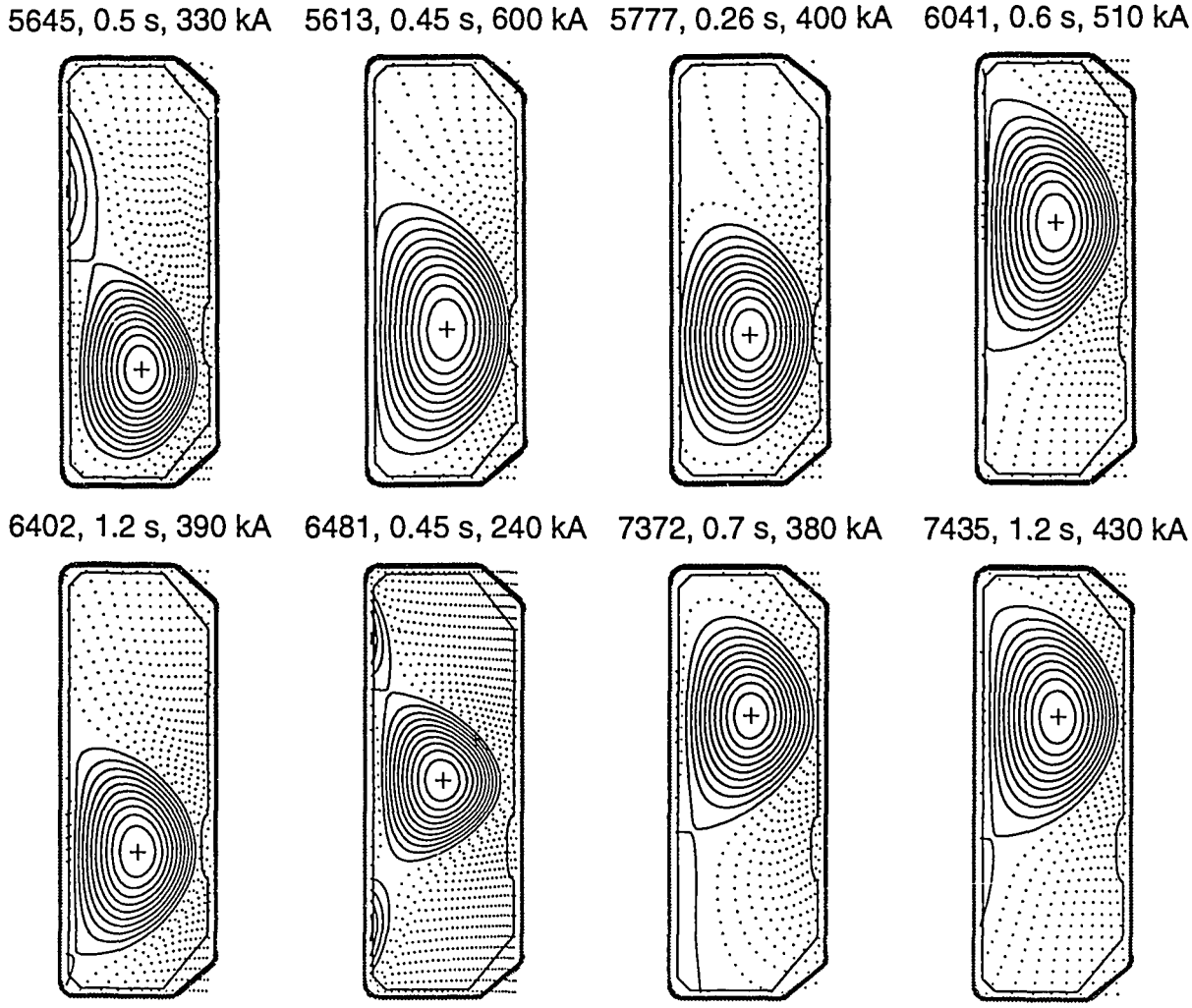

Figure 1. Selection of H-mode configurations produced in TCV

2. Evolution of Ohmic H-modes

The typical Single Null (SN) discharge 5645 in figure 1 illustrates most of the features observed in ohmic H-modes in TCV. The plasma current evolution is shown in figure 2 together, from top to bottom, with the vertically viewed D-alpha emission, the plasma line average density, the energy confinement time as obtained from magnetic reconstruction [Hofmann and Tonetti, 1988], the X-ray central temperature and the signal from a magnetic probe near the midplane on the high field side. Following the establishment of the complete magnetic configuration at 250 ms, the H-mode transition occurs at a density threshold ($3.5 \cdot 10^{19}$ m^{-3} in this case) after a period of hesitation (dither) which often includes ELM-like pulses of D_α emission and may be followed by a burst of type III ELMs. (The classification of ELMs follows that of Stambaugh et al. 1990). Ditherless transitions triggered by a sawtooth collapse have also been observed. In the example shown there is an initial ELM-free period, a short period of irregular 'mossy' ELMs causing low amplitude fluctuations on the D_α signal, followed by several 'Large ELMs', reminiscent of type I ELMs. The Large ELMs significantly reduce the energy confinement time and stabilize the density. This H-mode returned to L-mode and disrupted after a final period of mossy ELMs. The majority of ELM-free H-modes terminates with disruptions at the density limit, sometimes near the Greenwald limit. Stationary conditions of a duration equal to the entire current flat top (~1.5 s), have been obtained in H-modes with both Large and type III ELMs (figures 3a & 3b). The evolution of a limiter H-mode

is shown in figure 3c. Limiter H-modes have been obtained at high elongation (κ=1.7-1.9) and for plasma currents in the range 360-600 kA. Examples are given in figure 1 (shots 5613 and 5777).These discharges were limited on the carbon tiled inner wall, with a small gap (~1cm) between last closed flux surface (LCFS) and the belt limiter at the low field side. They had an X-point well outside the LCFS (9-17 cm). The poloidal flux between the X-point and the LCFS amounted to 4-12% of the flux inside the LCFS, depending on the configuration. These Limiter H-modes had fairly high threshold densities ($7\text{-}8\cdot10^{19}$ m^{-3}) and attained densities as high as $1.7\cdot10^{20}m^{-3}$. At 360 kA the limiter H-mode has been obtained only for $\delta > 0.25$, indicating that, in addition to high elongation, high triangularity is favourable for obtaining H-modes.

Until the end of 1994, all TCV discharges had been produced with both I_p and B_T positive (anticlockwise when viewed from above the machine), such that the ion grad_B drift was upwards. In 1995, after a major shutdown, H-modes have been produced with both directions of B_T and I_p. Single-Null H-modes obtained in the upper half of the vessel and $B_T < 0$, including mirror images of several configurations which produce ELMy H-modes with $B_T > 0$, are almost all ELM-free (figure 3d), irrespective of the sign of I_p. The differences may be the consequence of possible top/bottom asymetries, such as the presence of a belt limiter in the lower half of the vessel or asymetric error fields, rather than being directly linked to the the sign of B_T.

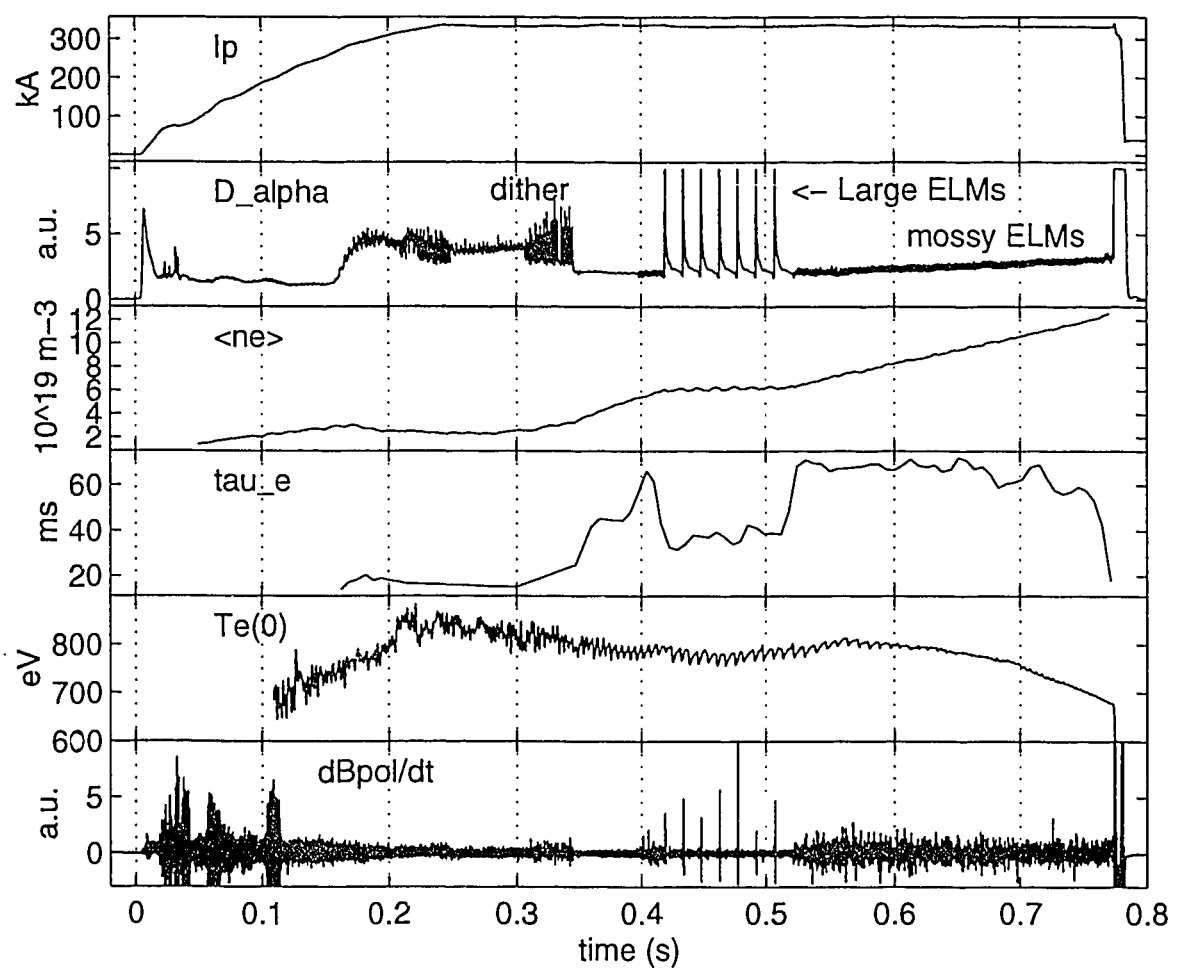

Figure 2. Evolution of ohmic H-mode in SN configuration (#5645).
From top to bottom: Plasma current, D_α monitor signal, line average density, confinement time, central temperature from an X-ray measurement and signal from HFS magnetic probe.

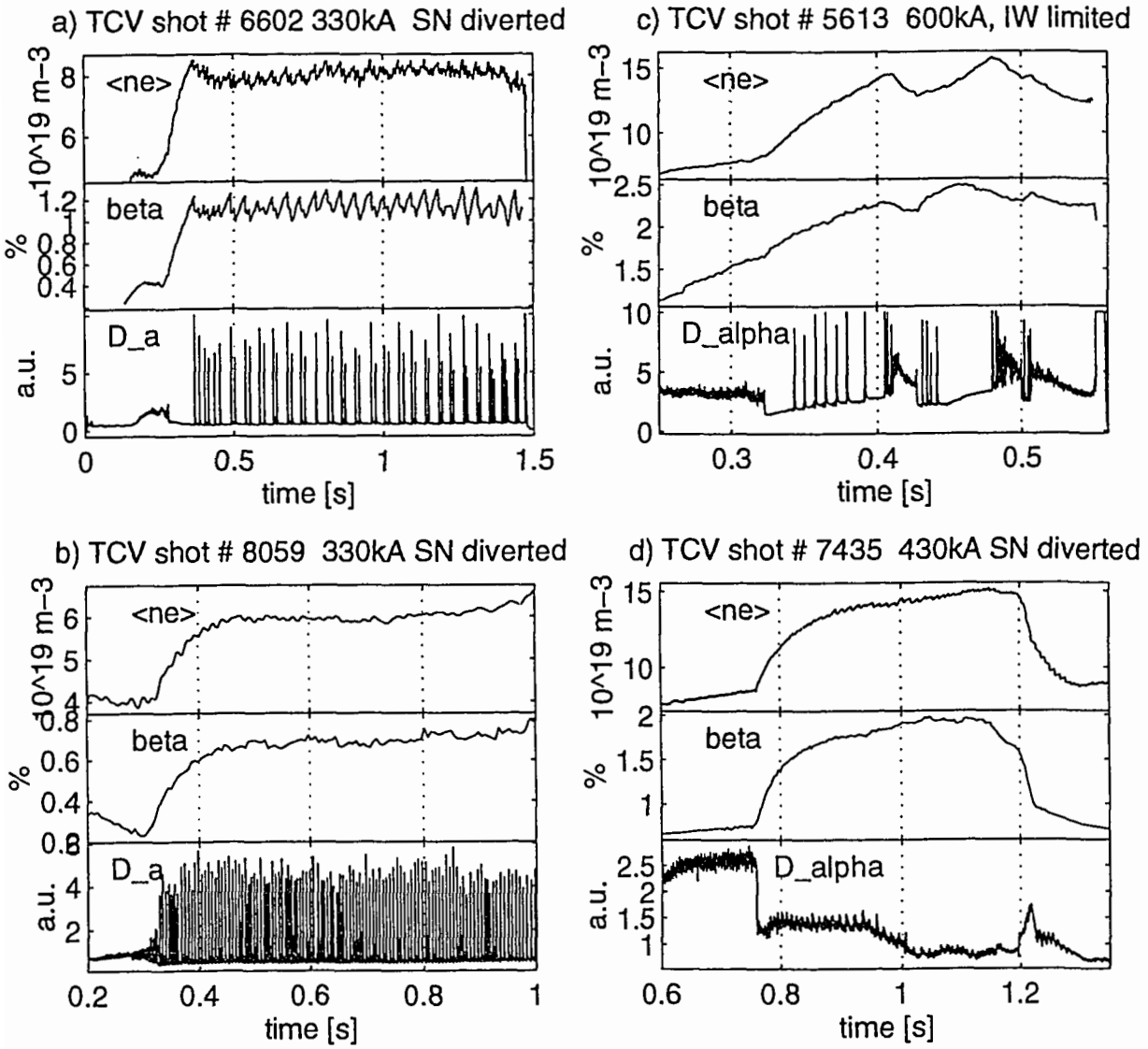

Figure 3. Examples of ohmic H-mode evolution in TCV
a) SN with Large ELMs
b) SN with type III ELMs
c) Limiter H-mode
d) SN ELM-free H-mode with $B_T<0$, $I_p>0$.

Edge temperatures of 200-300 eV, as compared to ~100 eV in L-mode, are measured in H-modes within 2-4 cm of the last closed flux surface (LCFS) by Thomson scattering. The X-ray emission near the edge ($r/a \geq 0.9$) increases by two orders of magnitude within 100 ms in ELM-free H-modes. Following the L-H transition the edge density measured by the FIR interferometer and by Thomson scattering rises rapidly by a factor of two (figure 4). These observations demonstrate the formation of an edge confinement barrier recognized as the most important characteristic of the H-mode since its discovery [Wagner et al, 1984]. Immediately after the transition, the density profile is extremely flat or slightly hollow. During the subsequent evolution, the temperature profile remains fairly constant while the density profile becomes more peaked.

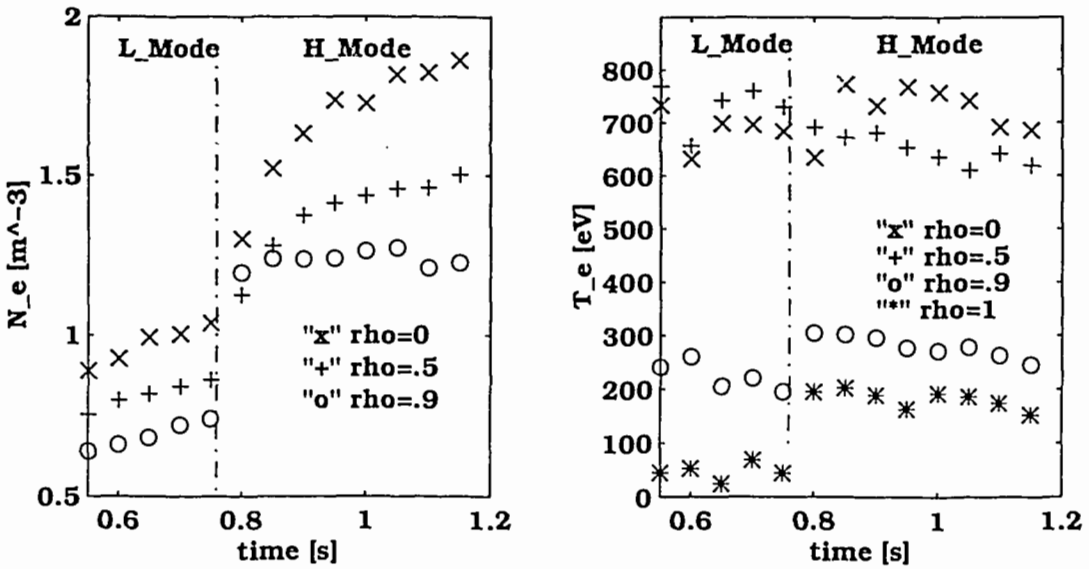

Figure 4. Electron density (left) and temperature (right) profile evolution in ELM-free H-mode measured by Thomson scattering. 'X' symbols refer to plasma center, '+' to mid-radius, circles to 90% of the minor radius, stars to r ≡ a±2cm. TCV discharge # 7435.

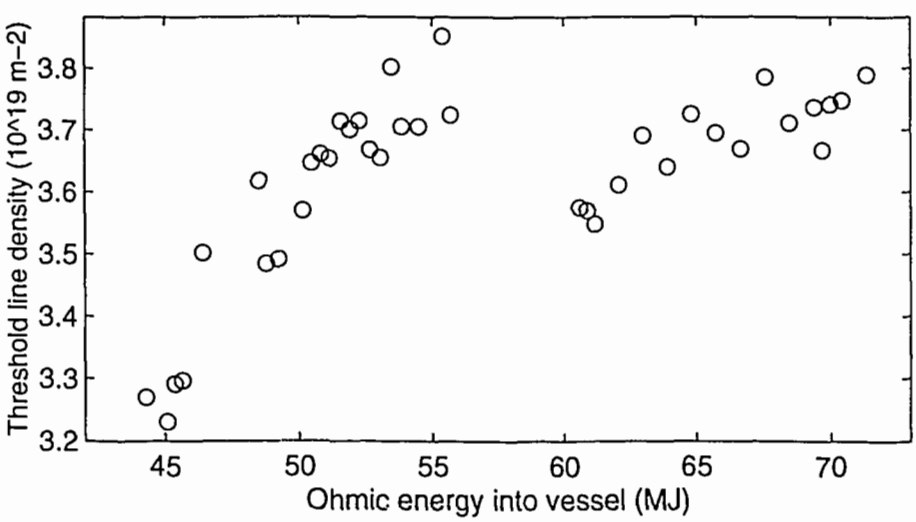

Figure 5. H-mode density threshold evolution over two experimental campaigns in DND configuration as function of ohmic energy deposited into the TCV vessel since the last boronization.

3. H-mode Threshold

A density threshold (in the range 3.5 - $8{\cdot}10^{19}$m^{-3}) is observed for the H-mode transition (Hofmann et al. 1994). The density threshold depends on the magnetic configuration, not however on the plasma current for a given configuration, provided the current (or ohmic power) exceeds a threshold to obtain an H-mode at all.

Throughout the 1994 and 1995 campaigns, for a given configuration and plasma current, the value of the density threshold varied by a factor of 2 depending on the history of plasma operation and vessel conditioning procedures (Duval et al. 1995). An example is shown in figure 5, which shows the density threshold evolution over two experimental campaigns with the same DND configuration (such as shot 6402 in figure 1), as a function of time integrated

ohmic power deposited into the vessel since the last reboronization. There was no glow discharge cleaning for the entire period shown. In both campaigns the density threshold increases slowly from discharge to discharge. The faster increase in the first series may be due to the large number of disruptions observed, while the second series was almost disruption-free. The two campaigns were separated by a series of L-mode limiter discharges centered at the vessel midplane, which appear to have had an effect of reconditioning of the vessel, possibly by spreading fresh boron onto the divertor area. The role of vessel conditions, particularly wall recycling, may be due to their influence on edge temperature (Snipes et al 1995).

4. Edge Localized Modes

Three types of ELMs have so far been observed on TCV (figure 6). Those occuring just after an L-H transition are almost certainly of type III. The nature of the Large ELMs observed after an ELM-free period is still unclear. We know of no counterpart on other experiments of the small 'mossy' ELMs.

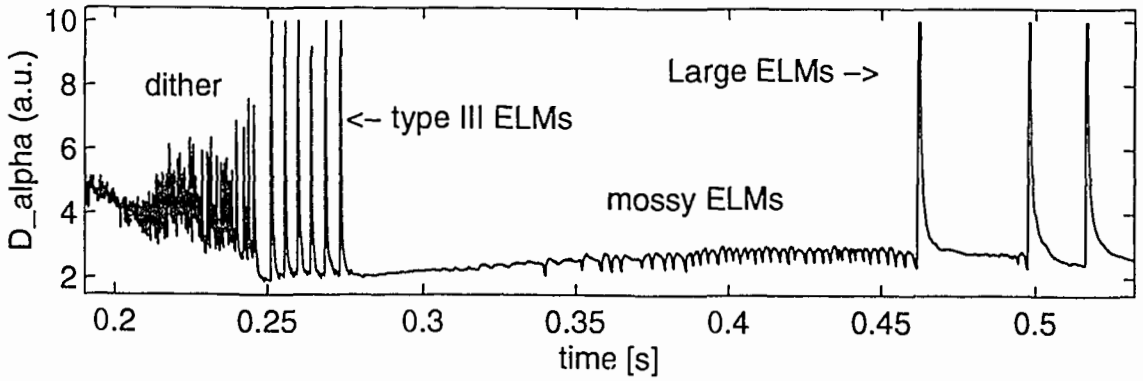

Figure 6. D_α signature for SN H-mode with type III, 'mossy' and Large ELMs (#5630).

Type III ELMs are observed just after an L-H transition with no or only a brief ELM-free period. Individual type III ELMs cause moderate reductions in particle content. The largest ELMs are observed after an initial ELM-free phase of 20 ms or more following the L-H transition in SN configurations. ELMs are seen on the magnetic probes as strong coherent magnetic pulses (fig. 2, bottom trace). The coherent component appears as a dominant m=1, n=0 (fast vertical displacement) together with an m=2,3, n=1 mode. Turbulent magnetic precursors beginning 0.1-3 ms before the D_α pulse have been observed in Double-Null D-shaped (DND) discharges (figure 7 a), but not before the Large ELMs occurring in SN discharges (figure 7 b). Distinct negative precursor signals beginning as much as 2 ms before the D_α emission maximum and the magnetic pulse, (figure 8) have also been observed on the floating potentials of Langmuir probes located at or near the high field side strike point locations in DND discharges [Pitts et al. 1994, 1995]. The signals in figure 8 are numerical 'box-car' averages over 20 ELMs, timed with respect to the peak of the D_α signal. Unfortunately no fast magnetic measurements, which may have shown the same precursors as in figure 7a, are available for these discharges.

Large ELMs have a significant impact on confinement (figure 9). In SN discharges ELMs can expell up to 12% of the stored energy and 7% of the particle inventory. At this level of perturbation the entire equilibrium, in particular position and edge safety factor, q_{95}, are affected by the ELMs. The X-ray emission at the edge (r/a ~ 0.93, second trace in figure 9) rises at the arrival of heat pulses released by sawtooth collapses (top trace, figure 9) and falls as a result of the energy loss associated with each ELM (D_α emission on bottom trace). A single ELM causes the emission to fall by a factor of 2 within 0.1 ms. In recent X-ray measurements with improved resolution, inverted ELM signals, akin to inverted sawteeth, have been observed just inside the LCFS in SN. It is interesting to note that in ELMy H-modes these discrete MHD events (sawteeth and ELMs) appear to dominate the power balance at the edge transport barrier. For comparison the type III ELMs shown in figure 3b expelled only 2-3% of the particle

content and 5% of the stored energy. ELMs of moderate amplitude are also seen in Double-Null discharges.

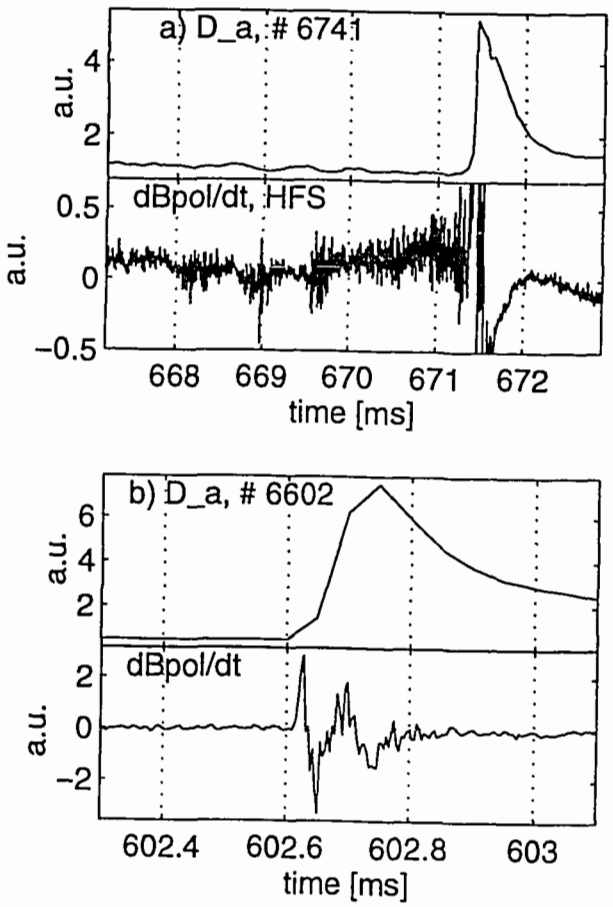

Figure 7. ELM precursors
a) DND configuration
top: D_α signal, bottom: HFS probe
b) as a) in SN configuration

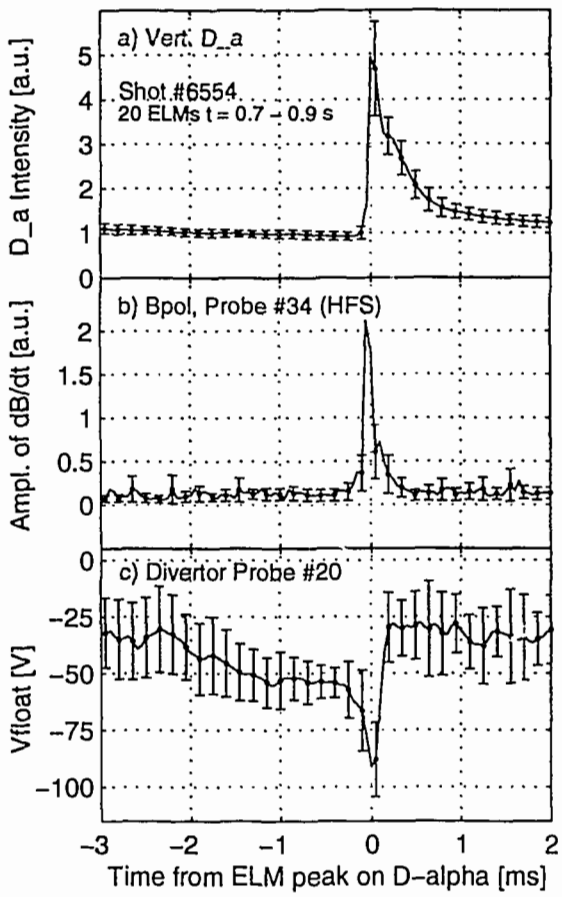

Figure 8. Floating potential precursors (DND)
a) D_α emission (averaged over 20 ELMs)
b) average amplitude of dB_p/dt
c) average floating potential

Large ELMs and type III ELMs transiently increase the neutral density in the plasma by a factor of 3-10, as shown in figure 10. The ELMs cause the signal from a vertically viewing Neutral Particle Analyser in the energy range 0.5-2.5 keV to rise proportionally to that of the D_α monitor. The ion temperature analysis, which uses the ratios from the different NPA channels, is practically unaffected, indicating that the resulting neutral density profile shape in the plasma is identical to the one established during ELM-free phases. The phenomenon may be due to neutral particles released from the tiles at the arrival of the ELM heat pulse or to charge exchange reactions of expelled particles with neutrals in the divertor.

The benign 'mossy' ELMs cause small (~10%) modulations of the D_α signals on detectors not viewing the X-point(s) (Pochelon et al 1994). A peculiar feature of 'mossy' ELMs is that they are initiated by a slow drop in the D_α emission (figure 11). The initial D_α level is then quickly restored with the magnetic pulse associated with the ELM. The strongest modulations, of order 100% in Double Null H-modes, are obtained on direct X-point views. On X-point views the emission overshoots the initial D_α level. The associated magnetic signature is also strongest near the X-points. These ELMs have not been observed for line average densities below $4.9 \cdot 10^{19} m^{-3}$. Mossy ELMs do not prevent the density rise typical of otherwise ELM-free H-modes, nor is there a noticeable reduction of energy confinement.

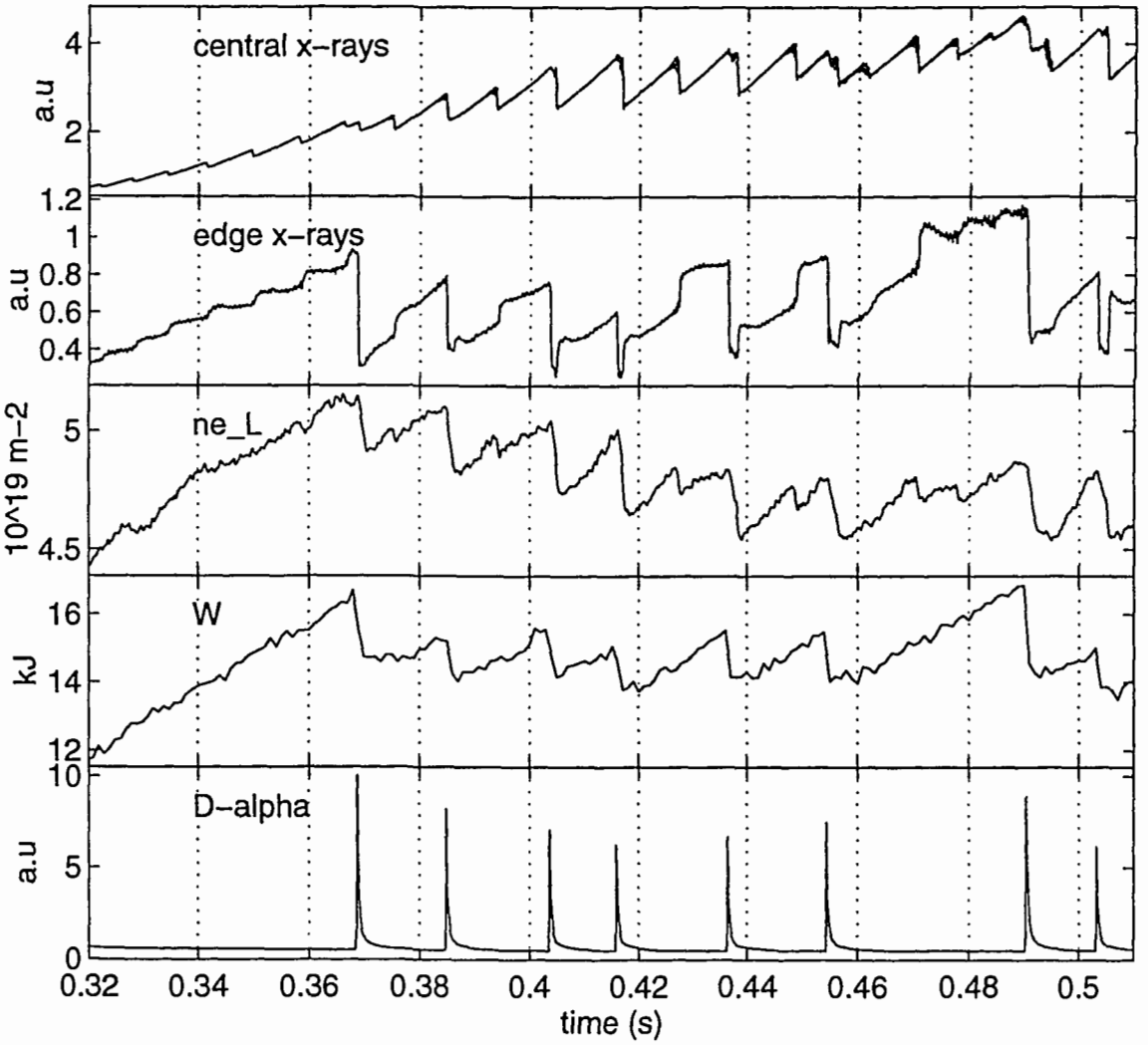

Figure 9. Effect of individual Large ELMs in a SN H-mode (shot # 6602)
From top to bottom: Central X-ray signal, edge X-ray signal, iine integrated density, stored energy, D_α monitor signal.

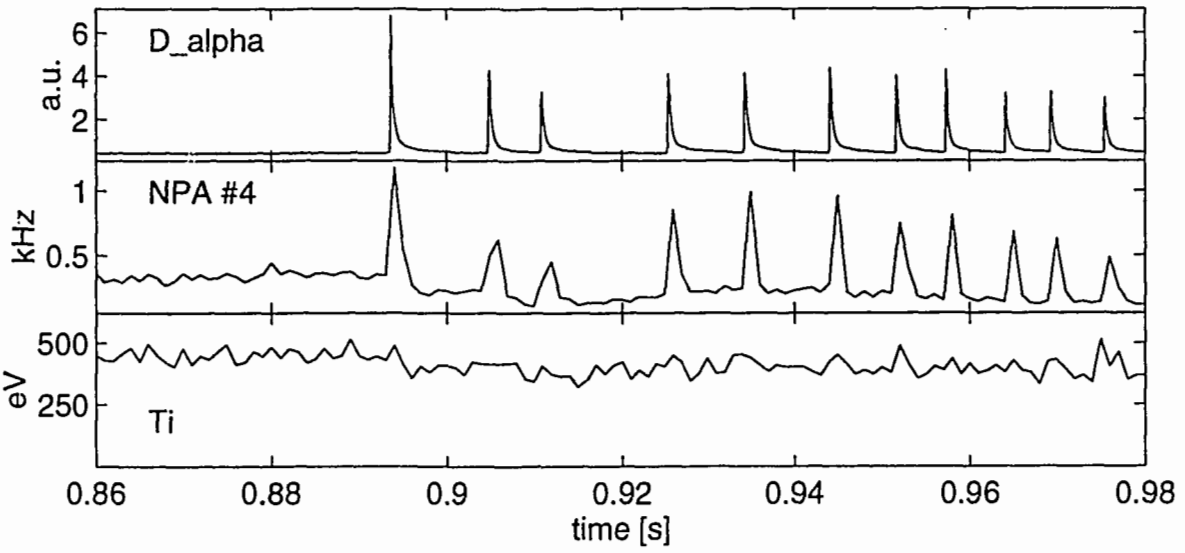

Figure 10. Charge exchange signals in ELMy H-mode. a) D_α monitor b) CX count rate for 1.6 keV channel of NPA c) Ion temperature from NPA measurement (TCV shot # 8001) .

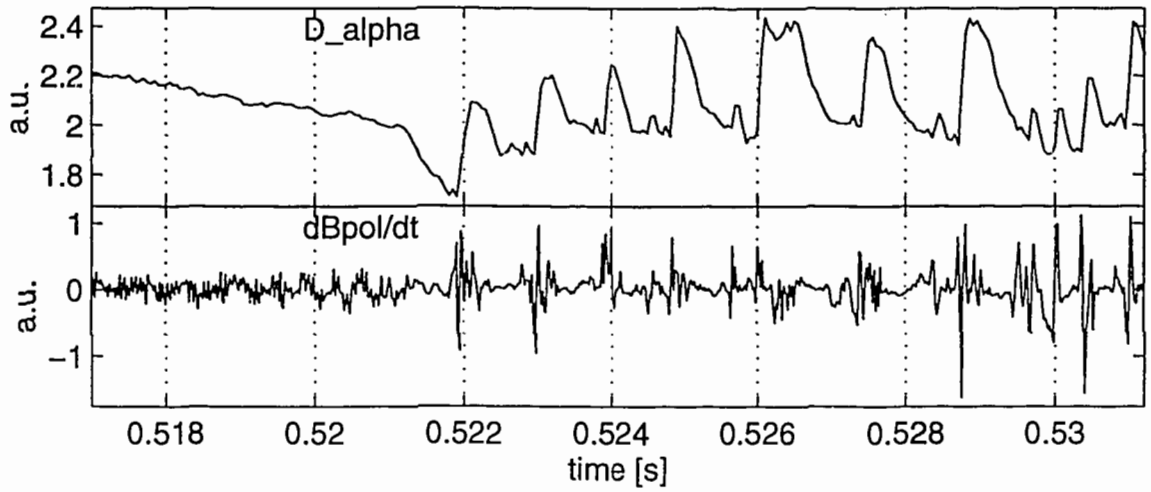

Figure11. D_α and magnetic signatures of 'Mossy' ELMs in a SN discharge (#5645).

5. ELM control experiments

In Double-Null D-shaped configurations, the presence of Large ELMs depends on whether the ion grad-B drift direction (upward) is towards (DND-T) or away from (DND-A) the 'active' X-point (Dutch et al. 1994). Switching between DND-T and DND-A was achieved by modulating the Ip·z reference signal. Figure 12 shows the result of such an experiment with a vertical shift of ± 1.2 cm. The most striking feature of figure 12 is the synchronisation of the ELM-free and ELMy phases with the imposed modulation. This relationship may be interpreted as due to the H-mode being closer to the threshold in DND-A, favouring the appearance of type III ELMs, as suggested by Zohm (1995a,b).

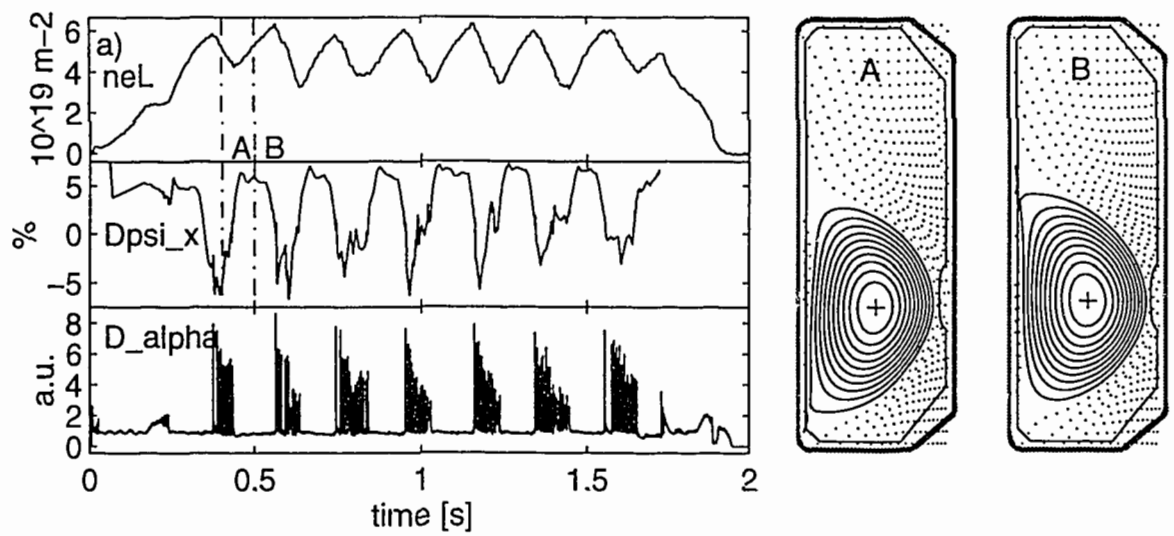

Figure12. a) Elm control experiment showing synchronization of ELMy phases with sign of DND X-point imbalance. Insert: DND-A and DND-T configurations. (#6181)

Results from DIII-D (Jackson et al, 1991) and JET (Stork et al, 1994) show that ELM behaviour strongly depends on plasma shape. A strong dependence on configuration has also been found in an (ongoing) experiment on TCV in which the lower and upper triangularities of SN H-modes with $B_T > 0$ (such as figure 1, shot 5645) were varied in the range $-0.1 \leq \delta_L \leq 0.6$, $0.6 \leq \delta_U \leq 0.8$, with $1.5 \leq \kappa \leq 1.6$. At high triangularity (or high elongation) Large ELMs, low ELM frequencies (f<100Hz, figure13a) and long (up to 0.4 s) ELM-free periods have been

observed. In the figures 13a and 13b near-stationary conditions characterized by $|d\langle n_e\rangle/dt|/\langle n_e\rangle < 1\ s^{-1}$ were selected. At low average triangularity, $\delta=1/2\ (\delta_L+\delta_U)$, or elongation ELMs were of high frequency (up to 400 Hz) with brief or no ELM-free periods. Unfortunately in the present dataset triangularity and elongation are correlated with the gaps between the LCFS and the vessel wall. Unexpectedly, the inner wall gap shows the best correlation with ELM behaviour (fig.13 b,c). The largest ELMs, longest ELM-free periods (figure 13c) and lowest ELM frequencies (< 100 Hz) are obtained with gaps wider than 2.2 cm (figure 3a). With smaller gaps H-modes have type III ELMs of relatively high frequency (figure 3b). The average particle and energy expulsion per ELM, $\langle\Delta N\rangle/N$ and $\langle\Delta W\rangle/W$, for groups of ELMs, was estimated from the respective balance equations as described in a separate paper (Weisen et al. 1995). Figure 13d shows that $\langle\Delta N\rangle/N$ increases with gap, from near 2% to near 7%, as the gap is varied from 1.2 to 3 cm. The symbols refer to classes of $\langle\Delta W\rangle/W$ ranging from 4% to 13%. There is a weaker correlation of $\langle\Delta W\rangle/W$ with gap width, however $\langle\Delta W\rangle/W$ is always larger than $\langle\Delta N\rangle/N$. In the presence of small high frequency ELMs the edge X-ray emission ($r/a \approx 0.9$) is 5 to 10 times lower than in the presence of the largest ELMs, reflecting large differences in edge pressure. It is interesting to note that there is a continuum of ELM frequencies and amplitudes ranging from clear type III ELMs to the largest ELMs. By contrast, mirror images in the upper half of the vessel, with $B_T<0$, of the configurations used in the above experiments, produced ELMs only transiently when the inner gap width was close to zero.

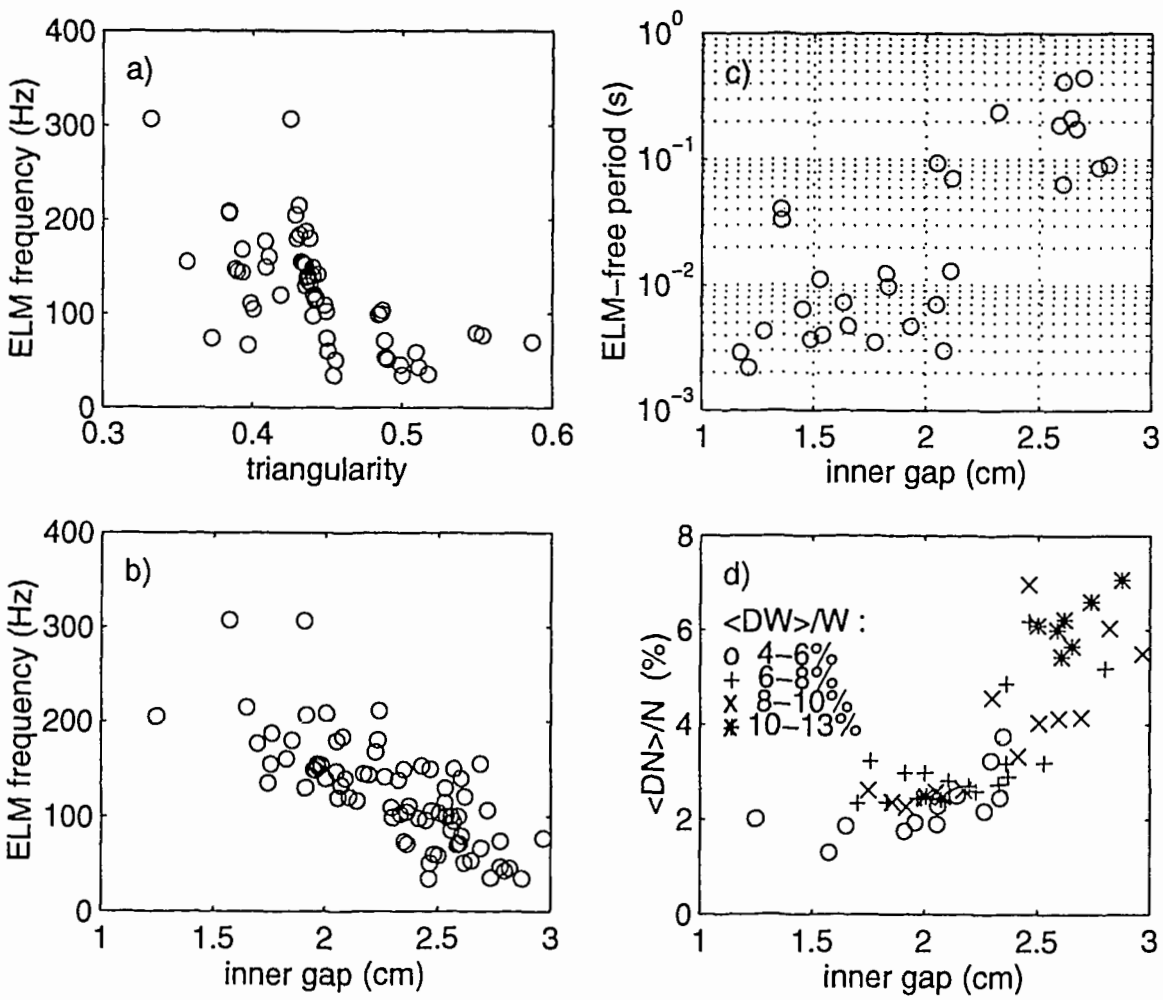

Figure 13. Effect of gap between inner wall and LCFS on ELM frequency and amplitude.
a) ELM frequency versus δ.
b) ELM frequency versus gap
c) Initial ELM-free period versus gap
d) ELM amplitude versus gap

6. Summary and conclusions.

In TCV, ELM behaviour is sensitive to configurational parameters such as the imbalance of a nominal Double Null plasma, the plasma-wall distance or plasma shape. This opens up the possibility of controlling both the H-mode evolution and the ELM amplitude. At present it is not clear to which degree configurational parameters influence the MHD stability directly and to what extent their influence is indirect, via their impact on plasma-wall interactions. ELM control has not been successful in all conditions. H-modes obtained with $B_T < 0$ in the upper half of the vessel have so far been refractory to attempts of inducing regular ELMs for obtaining quasi-stationary conditions.

A wide spectrum of ELM frequencies and amplitudes has been observed with $B_T > 0$ in the lower part of the vessel. The largest ELMs, which cause plasma particle losses of 7% and stored energy losses of 12%, have been observed in Single Null diverted discharges with a large (> 2.2 cm) plasma-to-wall distance. They occur after an ELM-free period of 20 ms or longer and have relatively low frequencies (≤ 120 Hz). As the plasma-wall separation is reduced the ELM amplitude decreases, their frequency increases (up to 400 Hz), the duration of the initial ELM-free period decreases and ELMs eventually occur without an initial ELM-free period, directly after the L-H transition. At this end of the spectrum they can be identified as type III ELMs. The largest ELMs, for which no obviuous precursor has yet been observed, are reminiscent of type I ELMs, although they may equally well be unusually large type III ELMs. Pending an unambiguous identification we refer to these as 'Large ELMs'. ELMs in the DND configurations, which are sensitive to X-point balance and hence to the H-mode threshold, are likely to be of type III. This is also supported by the observation of precursors in DND configurations. The importance of the plasma-wall separation suggests that recycling plays a key role in ELM behaviour, although we do not yet have direct evidence for this.

The observation of a continuum of ELM amplitudes and frequencies may be consistent with the picture sketched by Zohm (1995b) in which the edge plasma resistivity (and hence temperature) determines the critical pressure gradient at which ELMs become unstable. Type III and I ELMs form a continuum parameterised by edge plasma resistivity and bounded at its low resistivity end by type I ELMs. In ELM-free ohmic H-modes observed in TCV stabilization of type III ELMs may result from an increase of edge temperature due to the improved confinement, rather than from increased heating power as observed in devices with additional heating.

Acknowledgements. This work was partly supported by the Fonds National Suisse de la Recherche Scientifique. The authors wish to thank H. Zohm, F. Ryter and J. Snipes for stimulating discussions.

References.

Dutch M J, Hofmann, F, Duval B.P, Hirt A, Joye B, Lister J B, Martin Y et al. 1995 *Nuclear Fusion* **35**, 650

Duval B P, Martin Y, Dutch M J, Hofmann F, Lister J B, Moret et al 1995, *ECA Vol 19C, II-97*

Greenwald M, Terry J, Wofe S, Ejima S, Bell M, Kaye S, Neilsen G H 1988 *Nuclear Fusion* **28** 2199

Hofmann F. and Tonetti G. 1988 *Nuclear Fusion* **28** 1871

Hofmann F, Lister J.B, Anton M et al, *Plasma Phys. Contr. Fusion* **36**, 1994 B277.

Jackson G L et al 1991 *Phys. Rev. Lett.* **67** 3098

Pitts RA, Behn R, Chavan R, Duval B, Hofmann F, Lister JB, Weisen H *Bull. Am.Phys.Soc.* **39** (1994) 1757

Pitts RA, Hofmann F, Lister J B, Moret J M, Anton M, Burri A, Corboz M et al. 1995 *Euratom/DOE Workshop on Plasma Edge and Divertor Physics, Garching, Germany, 16-17 May.*

Pochelon A, Lister J B,Deschenaux Ch, Llobet X, Martin Y, Anton M et al 1995, ECA Vol 19C, IV-81

Pochelon A, Anton M, Bühlmann F, Dutch M J, Duval B P, Hirt A, Hofmann F et al 1994, ECA Vol 18C, III-1554

Snipes et al 1995, *this issue*

Stambaugh RD and the DIII-D Team 1990 IAEA CN-53/A-1-4

Stork D et al 1994 *Plasma Physics and Controlled Fusion* **36** A23

Wagner F, Fussmann G, Grave T et al 1984 *Phys. Rev., Lett.*, **53** 1453.

Weisen H, Dutch M J, Hofmann F, Martin Y, Moret J-M, Nieswand Ch, Pietrzyk Z A et al 1995 *this issue*

Zohm H 1995a *this issue*

Zohm H 1995b *'Edge Localized Modes', Review to be published in Plasma Physics and Controlled Fusion*

Effect on Confinement of Edge Localized Modes in TCV

H. Weisen, M.J. Dutch, F. Hofmann, Y. Martin, J.-M. Moret, Ch. Nieswand, Z.A. Pietrzyk, R.A. Pitts and A. Pochelon

Centre de Recherches en Physique des Plasmas, EPFL
Association EURATOM-Confédération Suisse, CH-1015 Lausanne

Abstract. The effect of ELMs on confinement in ohmic H-modes has been investigated by analysing the rates of change of global parameters such as the electron content and the stored energy as a function of ELM frequency. In Double Null H-modes ELMs are found to expell on average 2% of the electron content and 2.5% of the stored energy. In Single Null discharges which are separated by more than 2.2 cm from the inner wall, larger ELMs are observed which expell on average 3-7% of electron content and 3 to 12% of the stored energy. When the plasma-wall distance is reduced ELM frequencies increase and ELM amplitudes decrease. Quasi-stationary H-modes are obtained for $f_{ELM} \approx 130$ Hz in Double Null plasmas and f_{ELM} in the range 50-300 Hz in Single Null, depending on plasma to wall distance and ELM amplitude. The reduction in particle confinement due to the ELMs is sufficient to bring the ratio of particle to energy confinement times below 8 to 12 depending on ELM size and frequency.

1. Introduction

A general presentation of ELM behaviour in TCV ohmic H-modes is given in a separate paper [1]. Of the three kinds observed only 'Large ELMs' and type III ELMs, which have a clear influence on confinement, will be considered here. Large ELMs are observed after an ELM-free period of more than 20 ms following the L-H transition, while ELMs which can safely be identified as type III ELMs are seen immediately after the L-H transition or before an H-L transition. The largest ELMs observed to date have occurred in Single-Null (SN) discharges with a plasma to wall distance larger than 2.2 cm. Individual Large ELMs in these conditions can expell up to 7% of the plasma particle content and 12% of the stored energy (fig.9 in [1]). These ELMs are reminiscent of type I ELMs. In Double-Null D-shaped discharges (DND, such as shown in fig.12 in [1]) ELMs are normally too small to be individually resolved with our present diagnostics. The observation of turbulent precursors in DND suggests these ELMs are of type III.

2. Energy and particle balance in SN and DND discharges

The effect of ELMs on global confinement in ohmic H-modes has been investigated as a function of ELM frequency. We may take a time average (over many ELMs) of the usual particle balance and obtain

$$\langle dN/dt \rangle / N = \Phi_{in}/N - 1/\tau_{up} + f_{ELM} \cdot \langle \Delta N \rangle / N \qquad (1)$$

where the first term on the left hand side is the rate of change of the particle content averaged over a duration including many ELMs. τ_{up} stands for the underlying particle confinement time (applicable during intervals between ELMs) and Φ_{in} is the particle source, $\langle \Delta N \rangle$ is the average number of particles expelled per ELM (ΔN is negative) and f_{ELM} is the frequency of the ELMs. Analogous expressions hold for the impurity content, N_z, and the stored energy W. The effect of ELMs on confinement has been studied for a SN and for a DND configuration as function of ELM frequency. Examples are shown in figure 1 of [1], shots 5645 and 6402. In SN ELMs occurred spontaneously, whilst in DND they were controllable by adjusting the X-point imbalance. The experimental time traces were divided into windows with roughly constant ELM frequency, for which quantities of interest and their rates of change were sampled. The rates of change in electron content were measured using a 4 channel FIR interferometer and

stored energy was obtained from the equilibrium reconstruction. The rate of change of impurity content, assumed to be carbon, was estimated from a single chord X-ray measurement [2]. All rates of change vary nearly linearly with f_{ELM} up to a maximum frequency, ~300 Hz for DND and ~120 Hz for SN (figures 1 and 2; a,b,c). Above these frequencies smaller, irregular type III ELMs, compound ELMs and brief returns to L-mode are often observed in DND plasmas. The smaller irregular ELMs have been excluded from the present analysis. For an adequate estimate of ELM amplitude using equation (1) the source terms and the value of τ_{up} should be the same throughout the dataset. Since confinement correlates with density in ohmic plasmas, the density was windowed around the density at which stationary ELMy discharges were observed, $7 \cdot 10^{19} m^{-3} \leq \langle n_e \rangle \leq 10^{20} m^{-3}$. In order to limit the scatter in the particle source term, data with a closed gas valve were selected.

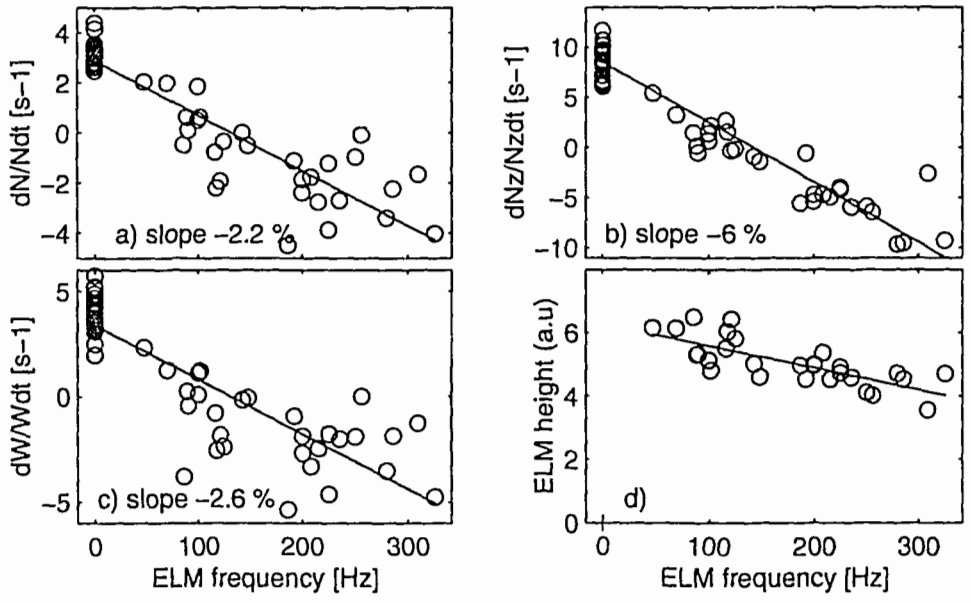

Figure 1. Rates of change of a) electron content, b) impurity content and c) stored energy versus ELM frequency in DND H-modes. d) pulse height of the D_α emission.

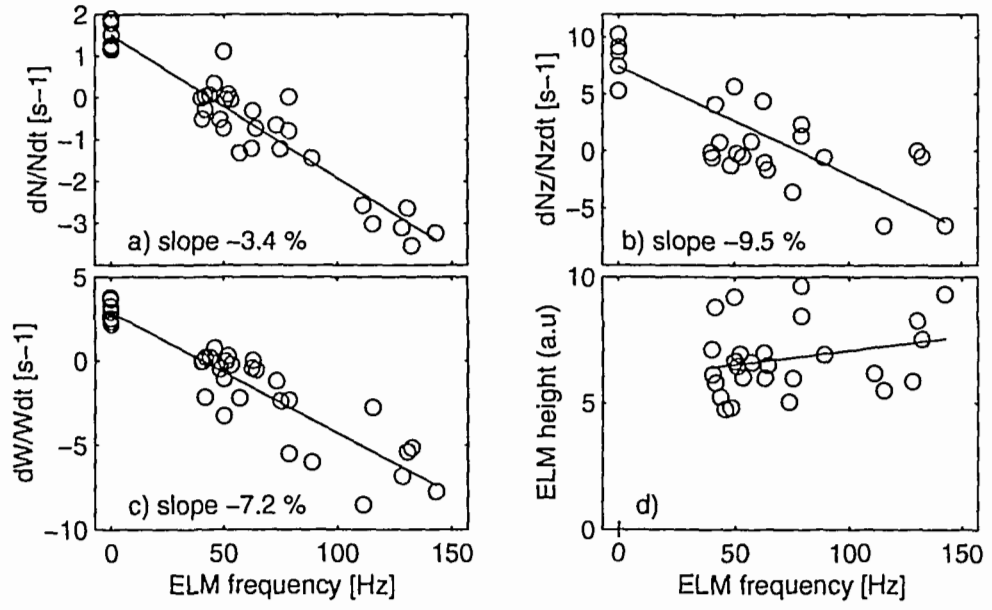

Figure 2. As figure 1, but for Single Null configuration

The method can provide $\langle \Delta N \rangle / N$ and $\langle \Delta W \rangle / W$ even if these quantities are functions of f_{ELM}. For the data shown straight lines were fitted, corresponding to the assumption of no dependence on f_{ELM}. The assumption is consistent with the observation that the average height

of the D_α pulse varies little as a function of f_{ELM} (figures 1.d and 2.d). From the slopes of the fitted lines we see that in DND these ELMs expel on average 2.2% of the electron content and 2.6% of the stored energy. In SN the corresponding numbers are 3.4% and 7.2%. These figures are in agreement with direct measurements with high time resolution in selected cases. The particle loss fraction should be taken as net since the gross outward flux caused by the ELMs may be partly offset by an influx due to ELM-enhanced recycling at the walls, as seen in neutral particle analyser measurements [1]. Using the same technique as described above for particle and energy content, it is also possible to determine fractional changes of other global quantities associated with an ELM event. In particular we found that both in SN and DND an average ELM causes a change in internal inductance and poloidal magnetic energy of about 1%.

The X-ray estimates for the impurity content are based on a single chord and cannot take into account profile changes due to the ELMs. The narrowing/broadening of the profiles during ELMy/ELM-free periods is expected to lead to an overestimate of the rate of change of impurity content. An overestimate is also expected in the presence of accumulation of impurities in the plasma core in ELM-free H-modes. Initial estimates using near infrared Bremsstrahlung, which are less profile sensitive, suggest the rates of change of impurity content, and hence $<\Delta N_Z>/N_Z$, are between those measured using X-rays ($<|\Delta N_Z|>/N_Z \sim 9\%$ in SN, 6% in DND) and those of the electrons ($\cong 3.4\%$ and 2.2%).

3. Confinement in stationary Elmy H-modes

The most attractive feature of ELMs is that they allow quasi-stationary H-modes if the product of ELM frequency and fractional loss is of the right magnitude. Since ELM size depends essentially on the chosen configuration, there is in each case a frequency $f_s = (\Phi_{in} - N/\tau_{up})/<\Delta N>$ at which the average rate of change is zero. In DND $f_s \approx 130$ Hz while in SN $f_s \approx 50$ Hz, due to the larger ELM size. Within errors the rates of change of all quantities investigated (including l_i) are zero at the same values of f_{ELM}, i.e. quasi-stationarity is obtained simultaneously with respect to all parameters investigated.

In the presence of ELMs the resulting average confinement times are given (from eq.1) by

$$\tau_p = \tau_{up}(1 - \tau_{up} f_{ELM} <\Delta N>/N)^{-1} \quad (2), \text{ and}$$

$$\tau_e = \tau_{ue}(1 - \tau_{ue} f_{ELM} <\Delta W>/W)^{-1} \quad (3)$$

for particles and for energy repectively. In stationary conditions $f_s<|\Delta W|>/W$ is about 3.6 s^{-1}, leading, for a $\tau_{ue} = 0.06$ s, to a 18% reduction in confinement time. The reduction compared to ELM-free H-modes of long duration (100 ms or more) is somewhat higher (~30%), probably because of differences in the plasma pressure profiles and hence in τ_{ue}. X-ray measurements near the plasma edge suggest that, even at the same average density, edge pedestals are smaller in the presence of ELMs. It is worth noting that since $\tau_{up} >> \tau_{ue}$ in ELM-free H-modes, the relative reduction in τ_p due to ELMs is much larger than the relative reduction in τ_e. It follows that $\tau_p/\tau_e < (\tau_{ue} f_{ELM} <\Delta N>/N)^{-1} + <\Delta W>N/<\Delta N>W$. This corresponds to $\tau_p/\tau_e < 8$ and 12 with the above figures for DND and SN respectively.

In a previously described experiment ([1], section 5) the triangularity and the distance ΔR_i between the plasma and the inner wall were varied in 330 kA SN plasmas to study their effect on ELM frequency and size. The frequency for stationary conditions (here defined by $-1s^{-1} \le <dN_e/dt>/N_e \le 1s^{-1}$), f_s increased monotonically from 40 Hz at $\Delta R_i = 2.8$ cm to 300 Hz at $\Delta R_i = 1.5$ cm (figure 13b in ref.[1]). The stationary density obtained decreases from typically $8 \cdot 10^{19} m^{-3}$ for $f_s = 50$ Hz to $5 \cdot 10^{19} m^{-3}$ for $f_s = 200$ Hz. These data were analysed as described above, except that figures of $<\Delta N>/N$ and $<\Delta W>/W$ were obtained for each group of ELMs analysed. (The number of samples for each configuration was to small for a comprehensive study such as shown in figures 1 & 2). This was possible because in ELM-free discharges dN/dt was practically constant, independently of plasma shape and density, when the gas valve was shut as is the case in figure 13d in [1]. For the estimate of $<\Delta W>/W$ we used

the circumstantial observation that dW/dt was inversely proportional to N for ELM-free H-modes of this dataset. For $\Delta R_i < 2.2$ cm type III ELMs with $<|\Delta N|>/N$ in the range 2-3% and $<|\Delta W|>/W$ near 5% were observed. For $\Delta R_i > 2.2$ cm Large ELMs with $<|\Delta N|>/N$ in the range 3-7% and $<|\Delta W|>/W$ of order 8% were observed. In all cases $<|\Delta W|>/W$ was larger than $<|\Delta N|>/N$. It is not clear what fraction of the expelled particles returns to the plasma as prompt recycling. If that fraction is less than about 50% the observation $<|\Delta W|>/W < <|\Delta N|>/N$ is inconsistent with a model in which the ELM merely expells particles outside a critical radius $r_c < a$, together with the contained thermal energy. If this were the case the fractional energy expulsion would be smaller than the fractional particle expulsion by a factor of the order of $(T_e(r_c) + T_i(r_c))/«T_e + T_i» \sim 0.5$, where «» denotes an average over plasma volume. An enhancement of diffusive heat losses during the ELM event has indeed been observed on other experiments [3].

In figure 3 the confinement times from the magnetic equilibrium reconstruction obtained in this experiment are shown versus line average density $<n_e>$ for both ELM-free H-modes (circles) and near-stationary ELMy H-modes. The symbols refer to classes of f_s. ELM-free confinement times are in fair agreement with the ITER93H-P prediction for ELM-free H-modes [4] for $<n_e> \geq 7 \cdot 10^{19} m^{-3}$. A density scaling of τ_e is seen for stationary ELMy discharges (symbols), corresponding to 1.7 times Neo-Alcator scaling [5]. At high density ($n_e \sim 8 \cdot 10^{19} m^{-3}$), corresponding to the largest, lowest frequency ELMs, the confinement of stationary ELMy H-modes is about 75% of the ITER93H-P prediction for ELM-free H-modes.

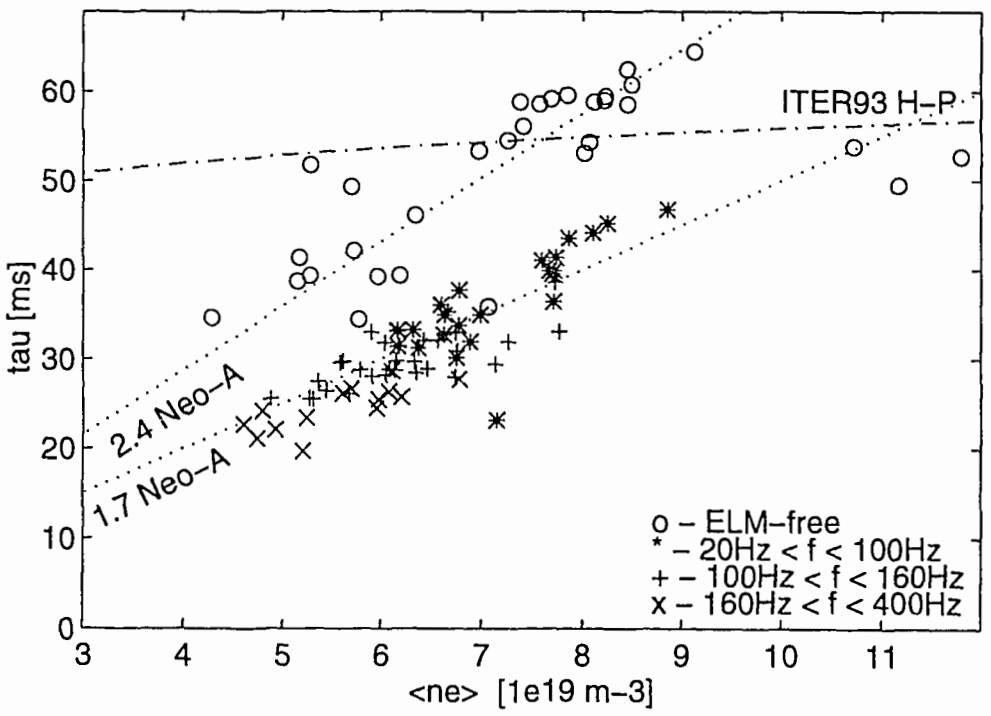

Figure 3. Energy confinement times versus line average density for Elm-free H-modes and for stationary ELMy H-modes in Single Null with Ip = 330 kA.

Acknowledgements: This work was partly supported by the Fonds National Suisse de la Recherche Scientifique. The support of many colleages is gratefully acknowledged.

References:

[1] Weisen H, F Hofmann, M J Dutch, Y Martin, A Pochelon, J-M. Moret, B P Duval et al. 1995, *this issue*
[2] H Weisen, D Pasini, A Weller, A Edwards, 1991 *Rev. Sci. Instrum* . **62** 1531
[3] Parail V et al 1994 *15th Int Conf Plasma Phys Cont Fusion Research,* IAEA-CN-60/A-2-II-3
[4] H-mode Database Working Group 1993 *Proc. 20ths EPS on CFPP, Lisbon* Vol. I, 103
[5] RR Parker, M Greenwald, SC Luckhardt, ES Marmar, M Porkolab, SM Wolfe 1985 *Nucl.Fusion* **25** 1127